Supporting Information

Impact of Imine Bond Orientations on Photocatalytic Hydrogen Generation of Benzothiadiazole-based Covalent Organic Frameworks Constructed using "Two-in-One" Monomers

Ze-Yang Wang,[†] Jia-Xin Guo,[†] Shuai Sun,[†] Chao-Qin Han,[*,†] Xiao-Yuan Liu[*,†]

[†] Hoffmann Institute of Advanced Materials, Shenzhen Polytechnic University, 7098 Liuxian Blvd, Nanshan District, Shenzhen, 518055, P. R. China

Chemicals

3,5-dibromobenzaldehyde, neopentyl glycol, *p*-toluenesulfonic acid, 4-(4,4,5,5-tetramethyl-1,3,2-dioxaborolan-2-yl)aniline, 4-(4,4,5,5-tetramethyl-1,3,2-dioxaborolan-2-yl)benzaldehyde, 3,5-dibromoaniline and 4,7-bis(4,4,5,5-tetramethyl-1,3,2-dioxaborolan-2-yl)benzo[*c*][1,2,5]thiadiazole were purchased from Shanghai Aladdin Biochemical Technology Co., Ltd. All the other chemicals were obtained from the chemical supplies and used without further purification.

Characterization

Nuclear magnetic resonance (NMR) data were collected using 400 MHz JEOL JNM-ECZ400S. Powder X-ray diffraction (PXRD) patterns were recorded using Bruker D8 Advance X-ray diffractometer with Cu Kα radiation. The photoluminescent and UV-vis absorption spectra were recorded on FLS1000 spectrofluorometer (Edinburgh Instruments) and Shimadzu UV-3600 spectrophotometer, respectively. Fourier transform infrared (FT-IR) spectra were recorded using a PerkinElmer spectrometer. The TGA data were obtained using TGA 550 (TA Instruments) analyzer and the samples were heated from room temperature to 800°C at a ramp rate of 10°C / min. Scanning electron micrographs (SEM) and Transmission electron microscope (TEM) images were taken using a JEOL JSM-IT800 (SHL) and Thermo Scientific Talos F200S, respectively. Gas chromatographic (GC) analysis was carried out on a CEAULIGHT GC-7920 instrument equipped with a thermal conductivity detector (TCD) using high pure nitrogen as the carrier gas.

Photoelectrochemical measurements

All the photoelectrochemical measurement were obtained on an electrochemical workstation

(CHI660E, CH Instrument Corp, Shanghai). 5 mg of HIAM-0026/HIAM-0026*v* was added to a mixed solution of 1 mL ethanol and 10 μL 5 wt% Nafion. The mixture was then ultrasonicated for two hours to get homogeneous suspension. The suspension was dropped on the surface of ITO glass and dried at room temperature. A standard three electrode system was used with the photocatalyst-coated ITO glass as the working electrode, Pt wire as the counter electrode and an Ag/AgCl as a reference electrode. 0.1 M Na_2SO_4 aqueous solution was used as the electrolyte. Mott-Schottky measurement was carried out at frequency of 1000, 1500 and 2000 Hz with amplitude of 5 mV.

Stability testing of COFs

Samples of HIAM-0026/HIAM-0026*v* (~ 5 mg) was suspended in 1 mL HCl solution (pH = 2, pH = 4), NaOH solution (pH = 10, pH = 12), water, or boiling water. These suspensions were sealed in 5 mL glass vials and stored at room temperature or 100 ℃ for 24 hours. The samples were then washed with ethanol and dried under 100 ℃ vacuum. The resultant COFs were used for PXRD and IR analysis.

Photocatalytic hydrogen evolution

3 mg HIAM-0026/HIAM-0026*v* was well dispersed in 50 mL deionized water containing 0.1 M ascorbic acid (AA) as the sacrificial agent. Then 0.018 M chloroplatinic acid (H_2PtCl_6) aqueous solution (3 wt% Pt) was introduced into the reaction system. The reaction solution was evacuated under vacuum to completely discharge air. After that the reaction system was irradiated vertically under 300 W xenon lamp with $\lambda > 420$ nm cut-off filter.

Apparent quantum efficiency (AQY) measurements were performed under monochromatic irradiation generated from a 300 W Xe lamp equipped with bandpass filters (central

wavelength: 450, 500 and 550 nm; full width at half maximum: 10 nm). Monochromatic photon fluxes at each wavelength were measured using an optical photodiode power meter (CEL-NP2000 Intense Light Power Meter). The corresponding intensities were 4.614, 9.536 and 5.906 mW cm^{-2}, respectively. The AQY was calculated using the following equation:

$$\eta_{AQY} = \frac{N_e}{N_p} \times 100\% = \frac{2 \times M \times N_A \times h \times c}{S \times P \times t \times \lambda} \times 100\%$$

Where, N_e is the amount of generated electrons, N_p is the incident photons, M is the amount of H_2 molecules (mol), N_A is Avogadro constant (6.022×10^{23} mol^{-1}), h is the Planck constant (6.626×10^{-34} J·s), c is the speed of light (3×108 $m \cdot s^{-1}$), S is the irradiation area (cm^2), P is the intensity of irradiation light ($W \cdot cm^{-2}$), t is the photoreaction time (s), λ is the wavelength of the monochromatic light (m).

Synthesis of 2-(3,5-dibromophenyl)-5,5-dimethyl-1,3-dioxane

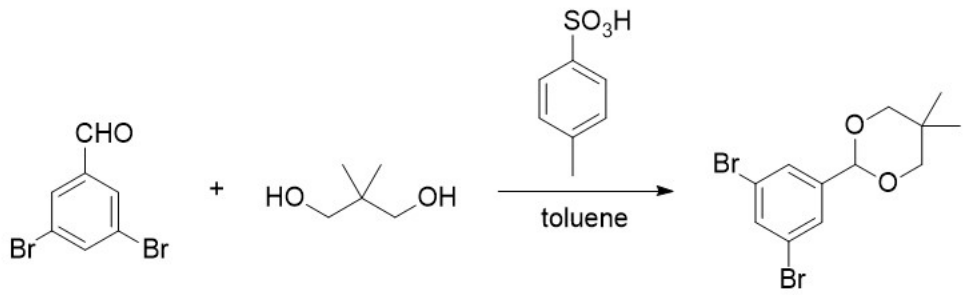

3,5-dibromobenzaldehyde (10.56 g, 40.00 mmol), neopentyl glycol (12.50 g, 120.00 mmol) and *p*-toluenesulfonic acid (0.68 g, 4.00 mmol) were added to a 500 mL of two-neck round-bottom flask. The reaction mixture was firstly deoxygenized with nitrogen for three times, and then 300 mL of toluene was added. The reaction mixture was heated 150 ℃ overnight under nitrogen. After cooling down to room temperature, the organic solvent was removed under reduced pressure to offer 2-(3,5-dibromophenyl)-5,5-dimethyl-1,3-dioxane as a white solid (14.00 g, yield: 99.0 %). ^{1}H NMR (400 MHz, $CDCl_3$) δ (ppm): 7.61 (1H), 7.56 (2H), 5.29 (1H), 3.73 (2H), 3.61(2H), 1.23 (3H), 0.77 (3H).

Synthesis of 3'-bromo-5'-(5,5-dimethyl-1,3-dioxan-2-yl)-[1,1'-biphenyl]-4-amine

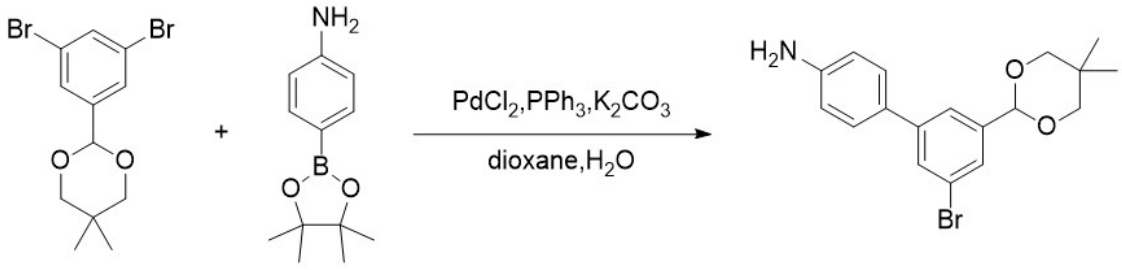

2-(3,5-dibromophenyl)-5,5-dimethyl-1,3-dioxane (40.00 mmol, 14.00 g), 4-(4,4,5,5-tetramethyl-1,3,2-dioxaborolan-2-yl)aniline (20.00 mmol, 4.38 g), $PdCl_2$ (1.00 mmol, 0.17 g),

PPh_3 (2.00 mmol, 0.52 g) and K_2CO_3 (40.00 mmol, 5.53 g) were added into one 500 mL flask containing 160 mL dioxane and 40 mL water. The mixture was degassed four times and stirred at 110 ℃ overnight under nitrogen. After cooling down to room temperature, the organic solvent was removed under reduced pressure. The crude product was purified by Al_2O_3 column chromatography to offer 3'-bromo-5'-(5,5-dimethyl-1,3-dioxan-2-yl)-[1,1'-biphenyl]-4-amine as a yellow solid (3.78 g, yield: 52.1 %). ^{1}H NMR (400 MHz, $CDCl_3$) δ (ppm): 7.63 (1H), 7.56 (2H), 7.38 (1H), 7.36 (1H), 6.71 (2H), 5.37(1H), 3.78 (2H), 3.64 (2H), 1.28 (3H), 0.79 (3H).

Synthesis of 5',5'''-(benzo[c][1,2,5]thiadiazole-4,7-diyl)bis(3'-(5,5-dimethyl-1,3-dioxan-2-yl)-[1,1'-biphenyl]-4-amine) (BTBBA)

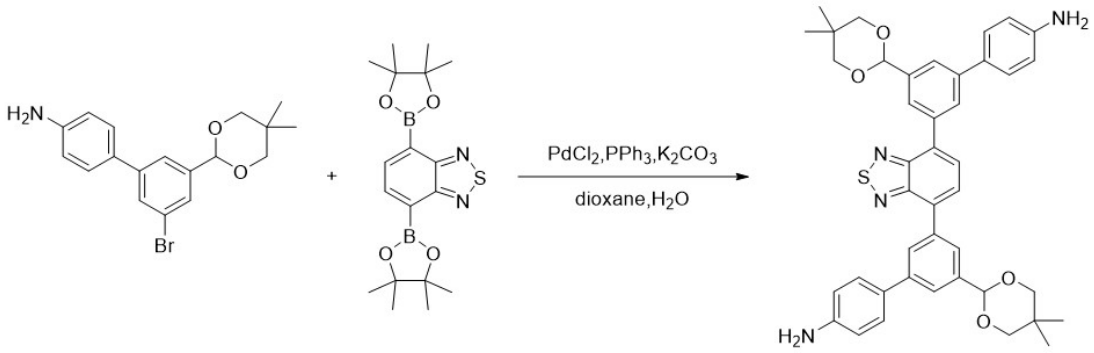

3'-bromo-5'-(5,5-dimethyl-1,3-dioxan-2-yl)-[1,1'-biphenyl]-4-amine (10.43 mmol, 3.78 g), 4,7-bis(4,4,5,5-tetramethyl-1,3,2-dioxaborolan-2-yl)benzo[*c*][1,2,5]thiadiazole (3.48 mmol, 1.35 g), $PdCl_2$ (0.34 mmol, 0.06 g), PPh_3 (0.69 mmol, 0.18 g) and K_2CO_3 (10.43 mmol, 1.44 g) were added into one 250 mL flask containing 80mL dioxane and 20 mL water. The mixture was degassed four times and stirred at 110 ℃ overnight under nitrogen. After cooling down to room temperature, the organic solvent was removed under reduced pressure. The crude product was

purified by Al_2O_3 column chromatography to offer 5',5'''-(benzo[c][1,2,5]thiadiazole-4,7-diyl)bis(3'-(5,5-dimethyl-1,3-dioxan-2-yl)-[1,1'-biphenyl]-4-amine) as an orange color solid (2.00 g, yield: 82.2 %). ^{1}H NMR (400 MHz, $CDCl_3$) δ (ppm): 8.19 (2H), 8.03 (2H), 7.89 (2H), 7.82 (2H), 7.58(4H), 6.82 (4H), 5.61 (2H), 3.87 (4H), 3.77 (4H), 1.38 (6H), 0.88 (6H). ^{13}C NMR (100 MHz, $CDCl_3$) δ (ppm):154.28, 146.12, 141.74, 139.41, 138.03,132.30, 132.20, 128.76, 128.64, 128.45, 125.16, 124.41, 115.53, 101.82, 75.18, 30.46, 25.00, 23.31, 22.09.

Synthesis of 2-(4-(5,5-dimethyl-1,3-dioxan-2-yl)phenyl)-4,4,5,5-tetramethyl-1,3,2-dioxaborolane

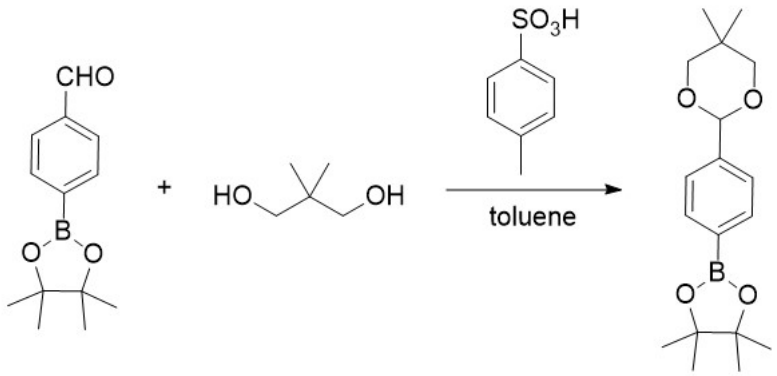

4-(4,4,5,5-tetramethyl-1,3,2-dioxaborolan-2-yl)benzaldehyde (4.64 g, 20 mmol), neopentyl glycol (6.25 g, 60.00 mmol) and *p*-toluenesulfonic acid (0.34 g, 2.00 mmol) were added to a 500 mL of two-neck round-bottom flask. The reaction mixture was firstly deoxygenized with nitrogen for three times, and then 300 mL of toluene was added. The reaction mixture was heated 150 ℃ overnight under nitrogen. After cooling down to room temperature, the organic solvent was removed under reduced pressure to offer 2-(4-(5,5-dimethyl-1,3-dioxan-2-yl)phenyl)-4,4,5,5-tetramethyl-1,3,2-dioxaborolane as a white solid (6.36 g, yield: 99.0 %). ^{1}H NMR (400 MHz, $CDCl_3$) δ (ppm): 7.78 (2H), 7.46 (2H), 5.38 (1H), 3.75 (2H), 3.63(2H), 1.27 (3H), 0.99 (6H), 0.88 (6H), 0.78 (3H).

Synthesis of 5-bromo-4'-(5,5-dimethyl-1,3-dioxan-2-yl)-[1,1'-biphenyl]-3-amine

2-(4-(5,5-dimethyl-1,3-dioxan-2-yl)phenyl)-4,4,5,5-tetramethyl-1,3,2-dioxaborolane (25.00 mmol, 7.96 g), 3,5-dibromoaniline (100.00 mmol, 25.09 g), $PdCl_2$ (1.25 mmol, 0.22 g), PPh_3 (2.50 mmol, 0.65 g) and K_2CO_3 (50.00 mmol, 6.91 g) were added into one 500 mL flask containing 200 mL dioxane and 50 mL water. The mixture was degassed four times and stirred at 110 ℃ overnight under nitrogen. After cooling down to room temperature, the organic solvent was removed under reduced pressure. The crude product was purified by Al_2O_3 column chromatography to offer 3'-bromo-5'-(5,5-dimethyl-1,3-dioxan-2-yl)-[1,1'-biphenyl]-4-amine as a yellow solid (2.10 g, yield: 23.1 %). ^{1}H NMR (400 MHz, $CDCl_3$) δ (ppm): 7.54 (2H), 7.50 (2H), 7.07 (1H), 7.80 (1H), 6.75(1H), 5.38 (1H), 3.78 (2H), 3.66 (2H), 1.29 (3H), 0.80 (3H).

Synthesis of 5,5''-(benzo[c][1,2,5]thiadiazole-4,7-diyl)bis(4'-(5,5-dimethyl-1,3-dioxan-2-yl)-[1,1'-biphenyl]-3-amine) (BTBBA*v*)

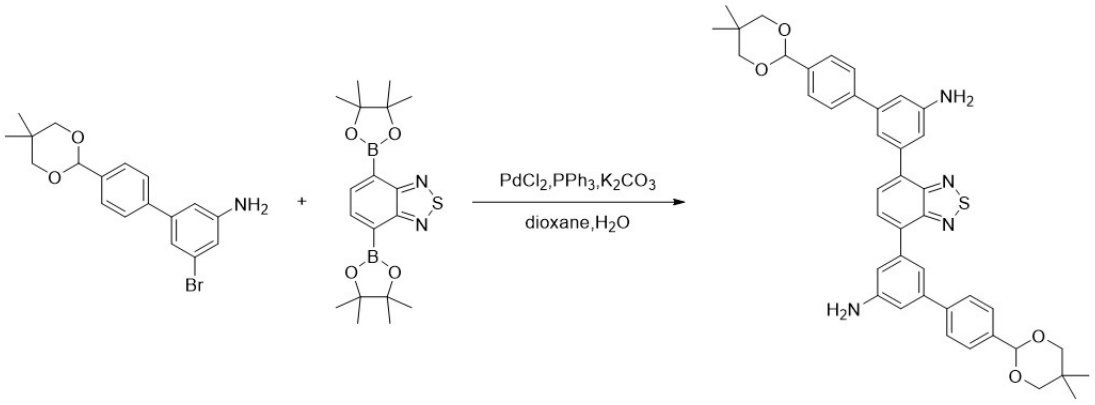

5-bromo-4'-(5,5-dimethyl-1,3-dioxan-2-yl)-[1,1'-biphenyl]-3-amine (12.70 mmol, 4.60 g), 4,7-bis(4,4,5,5-tetramethyl-1,3,2-dioxaborolan-2-yl)benzo[*c*][1,2,5]thiadiazole (8.47 mmol, 3.29 g), $PdCl_2$ (0.42 mmol, 0.07 g), PPh_3 (0.84 mmol, 0.22 g) and K_2CO_3 (16.93 mmol, 2.34 g) were added into one 250 mL flask containing 80mL dioxane and 20 mL water. The mixture was degassed four times and stirred at 110 ℃ overnight under nitrogen. After cooling down to room temperature, the organic solvent was removed under reduced pressure. The crude product was purified by Al_2O_3 column chromatography to offer 5,5''-(benzo[c][1,2,5]thiadiazole-4,7-diyl)bis(4'-(5,5-dimethyl-1,3-dioxan-2-yl)-[1,1'-biphenyl]-3-amine) as an orange color solid (1.80 g, yield: 30.43 %). ^{1}H NMR (400 MHz, $CDCl_3$) δ (ppm): 7.76 (2H), 7.64 (4H), 7.56 (4H), 7.49 (2H), 7.26(2H), 6.96 (2H), 5.43 (2H), 3.78 (4H), 3.66 (4H), 1.30 (6H), 0.77 (6H). ^{13}C NMR (100 MHz, $CDCl_3$) δ (ppm):154.16, 147.00, 142.54, 141.92, 139.01, 137.73, 133.52, 128.18, 127.32, 126.61, 119.03, 115.23, 114.14, 101.67, 75.11, 30.35, 24.93, 23.16, 22.00

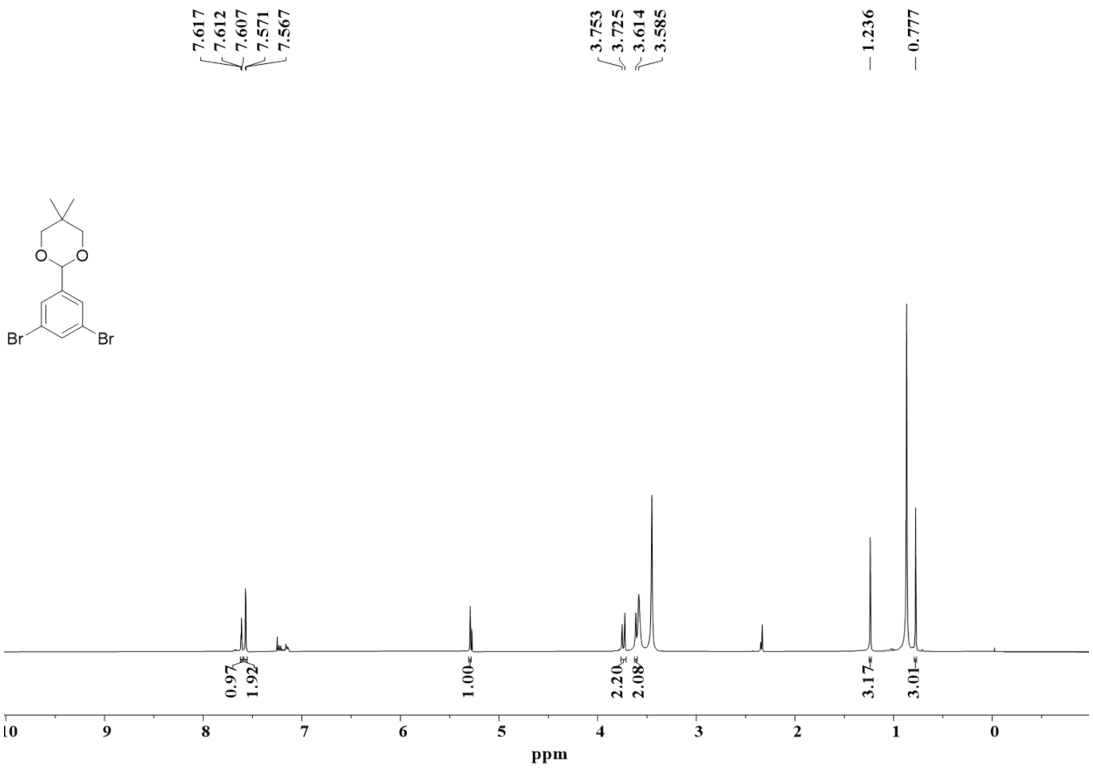

Figure S1. ^{1}H NMR spectrum of 2-(3,5-dibromophenyl)-5,5-dimethyl-1,3-dioxane.

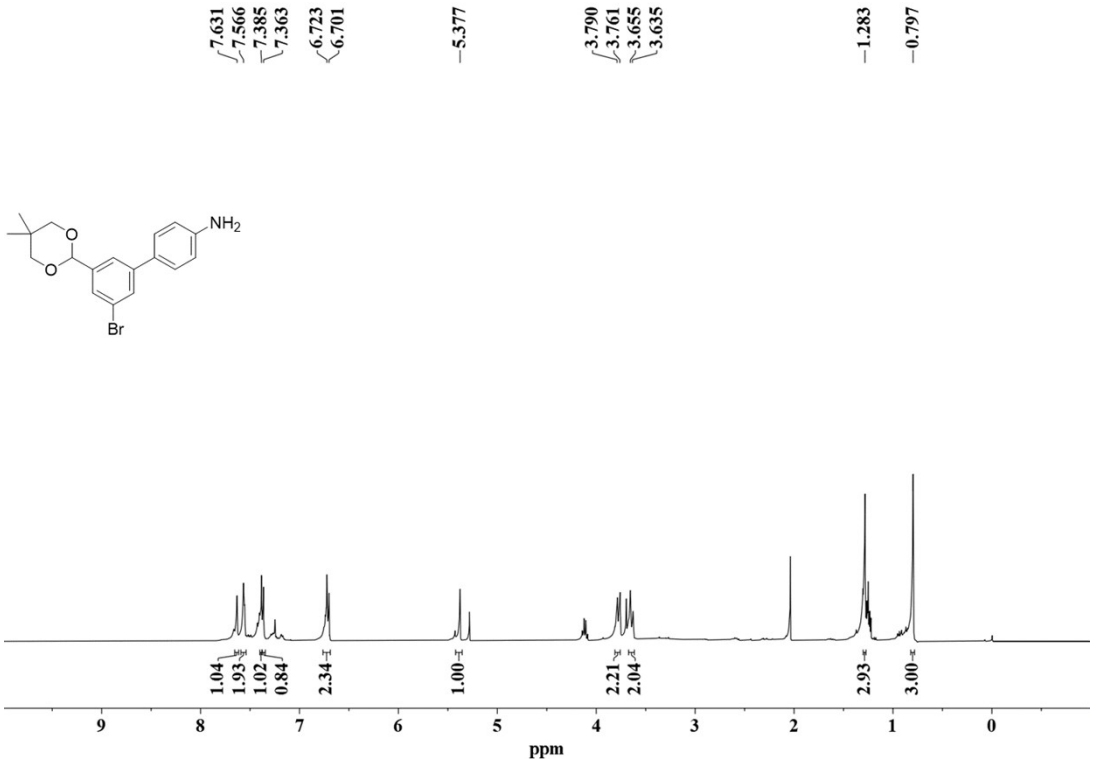

Figure S2. ^{1}H NMR spectrum of 3'-bromo-5'-(5,5-dimethyl-1,3-dioxan-2-yl)-[1,1'-biphenyl]-4-amine.

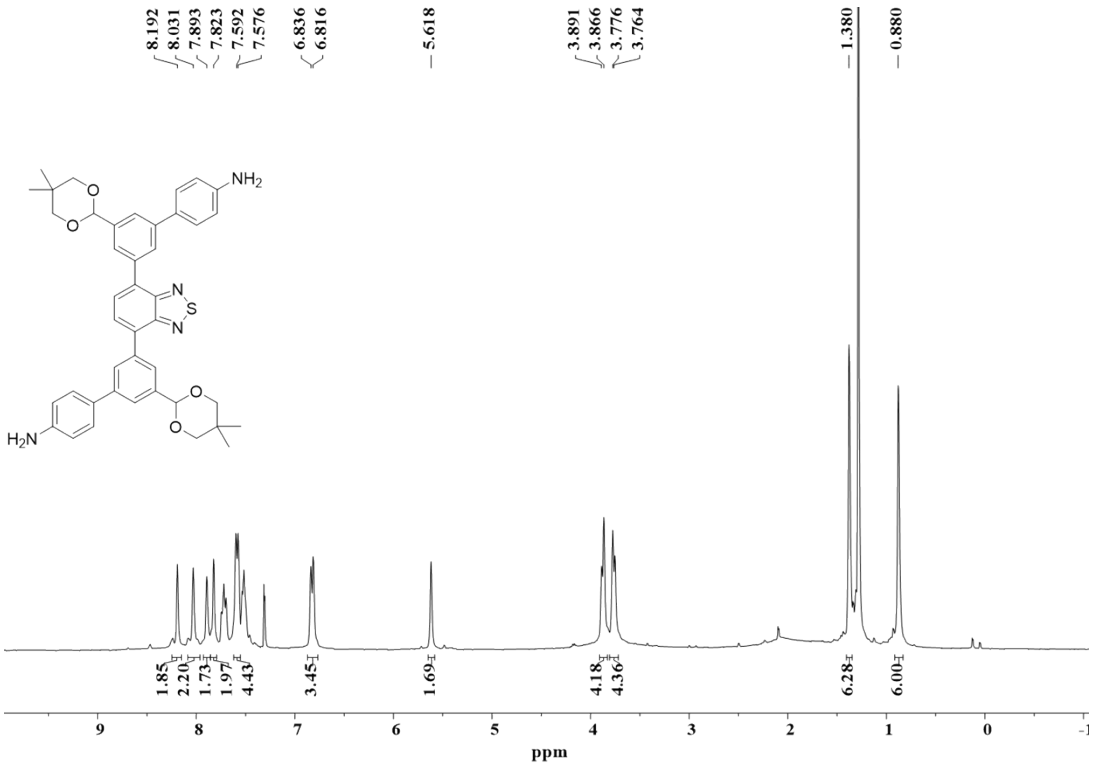

Figure S3. ^{1}H NMR spectrum of BTBBA.

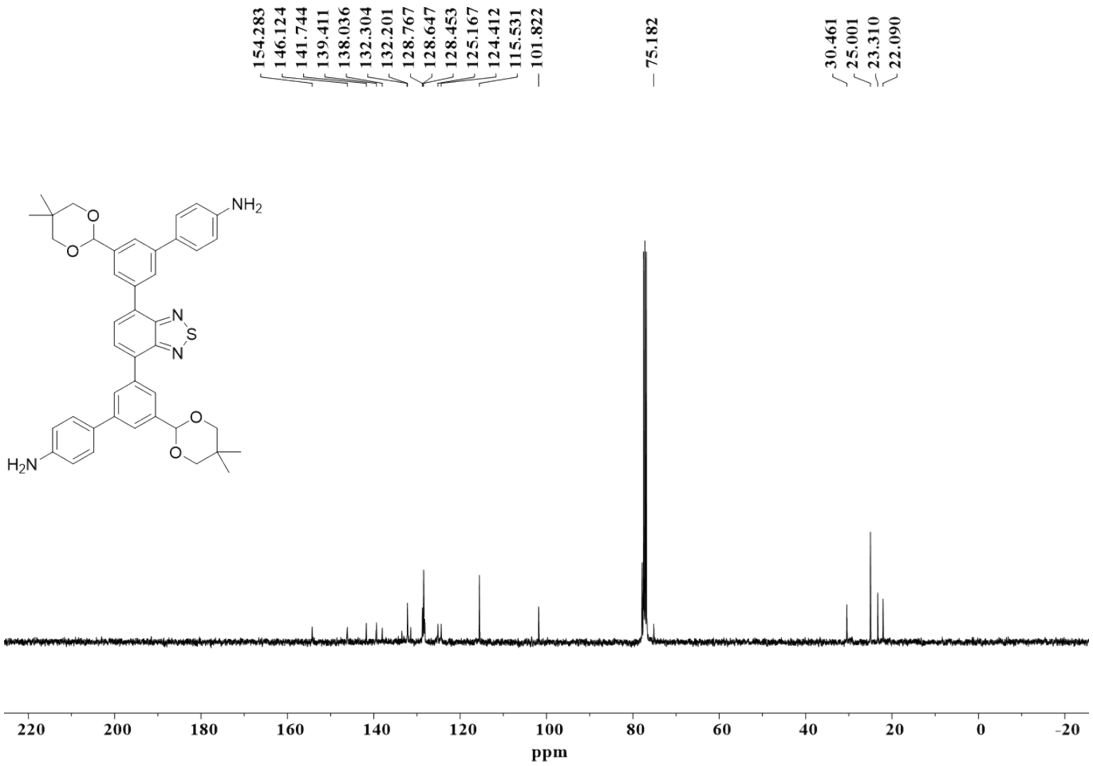

Figure S4. ^{13}C NMR spectrum of BTBBA.

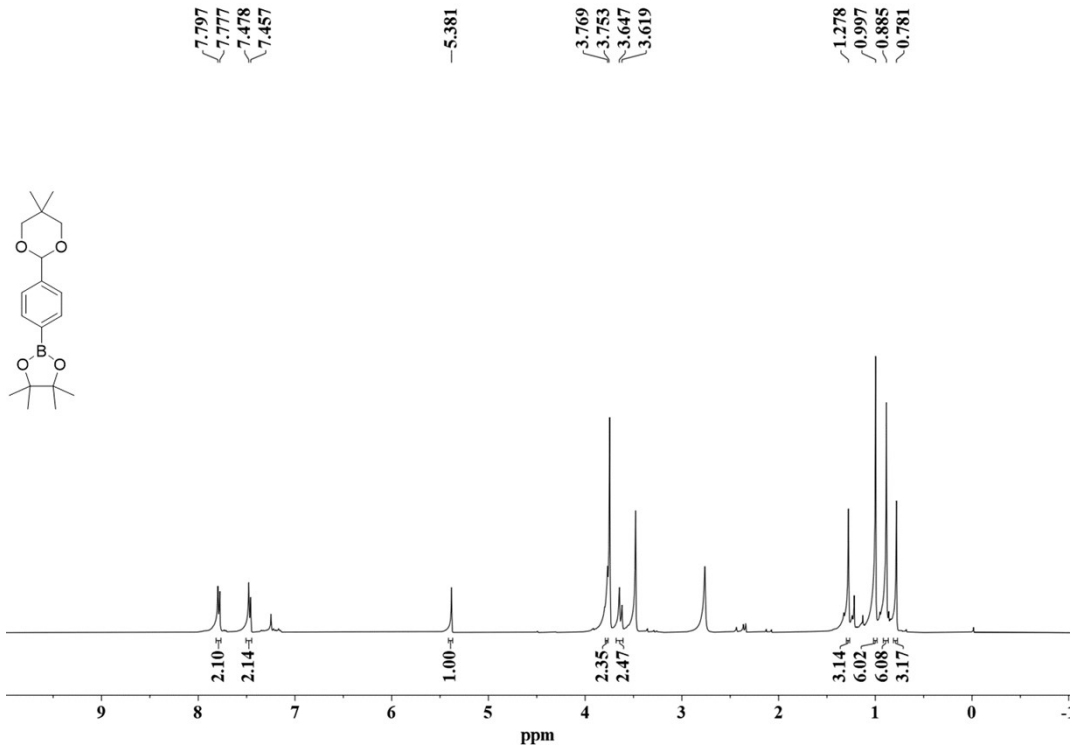

Figure S5. ^{1}H NMR spectrum of 2-(4-(5,5-dimethyl-1,3-dioxan-2-yl)phenyl)-4,4,5,5-tetramethyl-1,3,2-dioxaborolane.

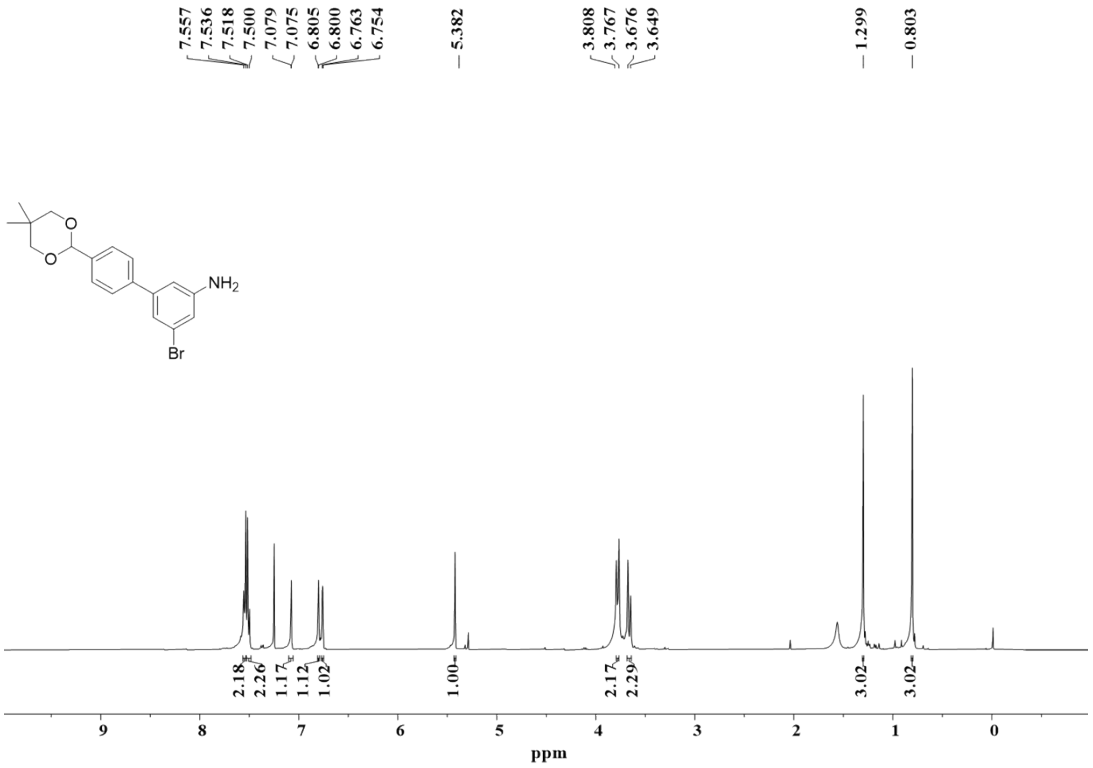

Figure S6. ^{1}H NMR spectrum of 5-bromo-4'-(5,5-dimethyl-1,3-dioxan-2-yl)-[1,1'-biphenyl]-3-amine.

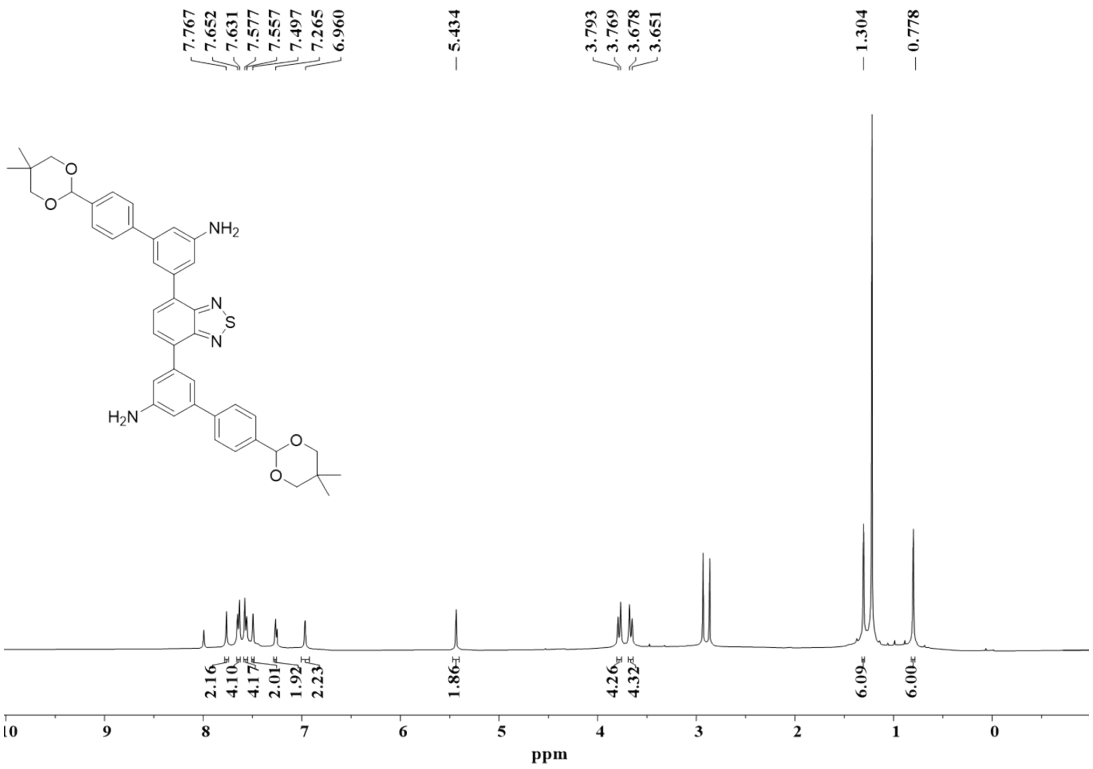

Figure S7. ^{1}H NMR spectrum of BTBBA*v*.

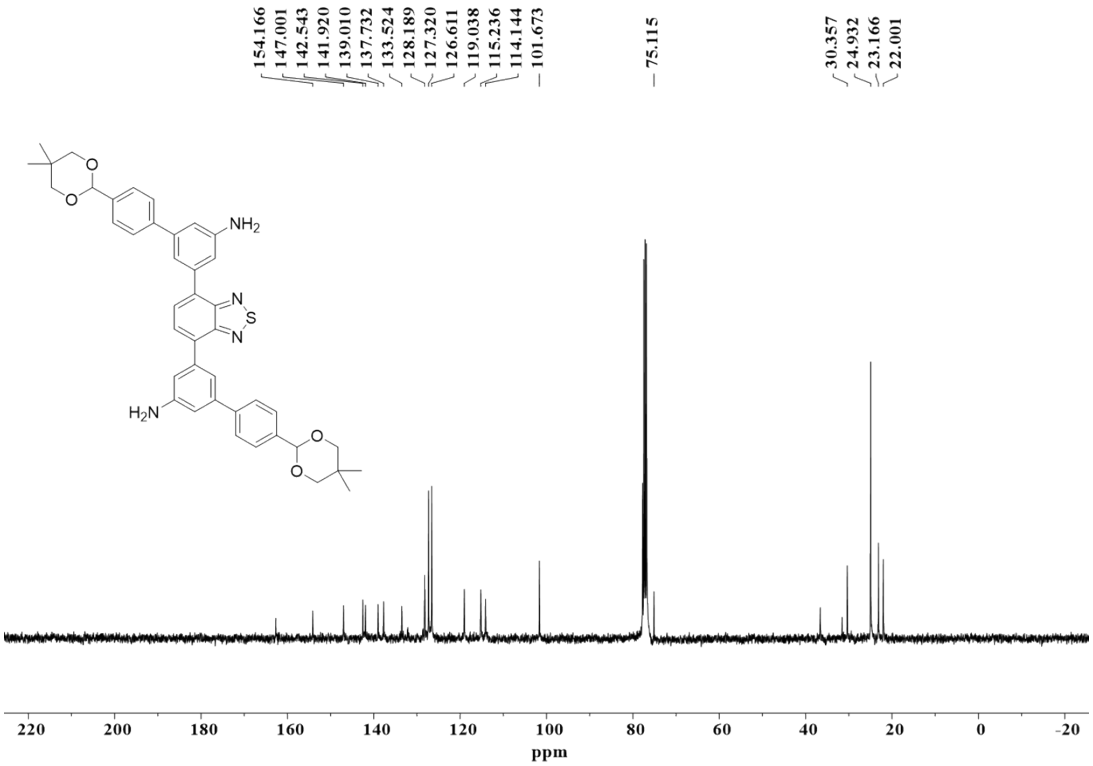

Figure S8. ^{13}C NMR spectrum of BTBBA*v*.

Synthesis of HIAM-0026

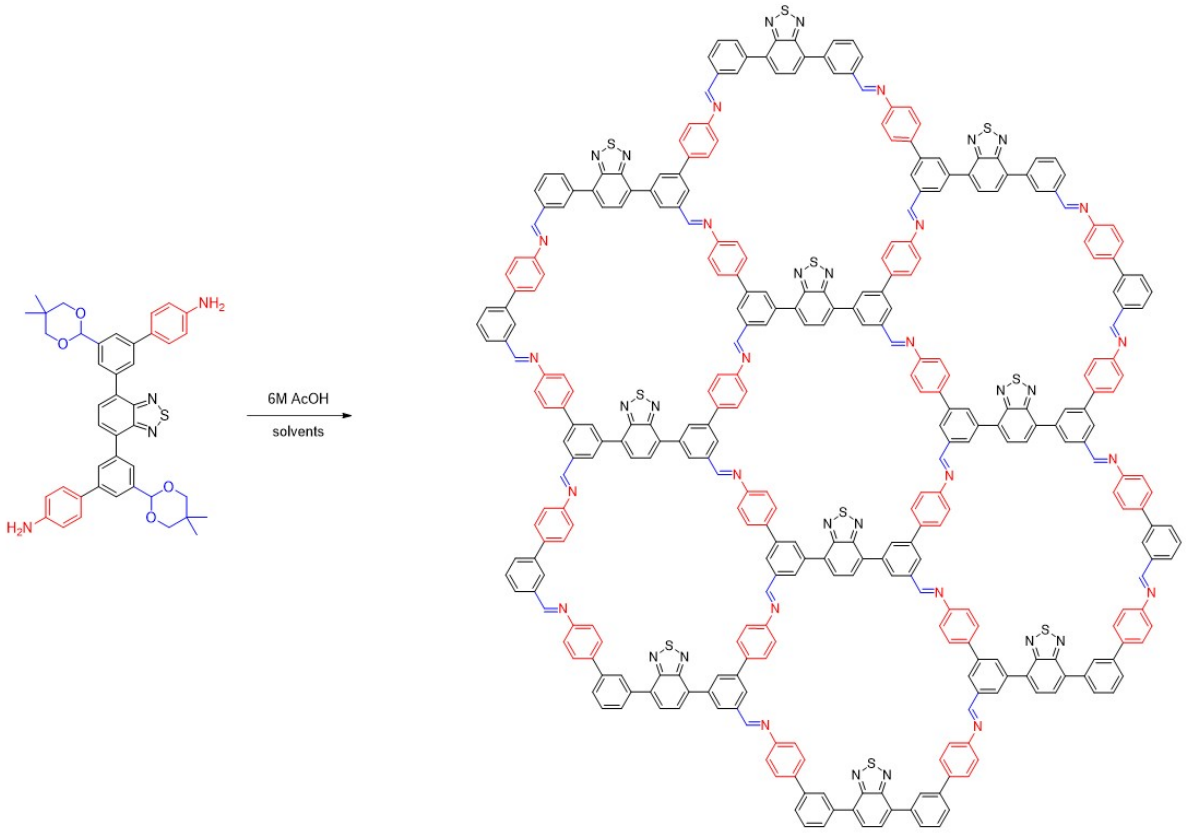

A Pyrex tube (10 mL) containing BTBBA (31.4 mg, 0.045 mmol) and *n*-butyl alcohol (*n*-BuOH, 1 mL) was sonicated for 3 min. Subsequently, 0.3 mL of acetic acid (6 M) was added. The tube was degassed through three freeze-pump-thaw cycles and then heated at 120 °C for 72 h. After cooling to room temperature, the precipitate was collected by filtration and washed with *N,N*-dimethylformamide (DMF) and ethanol (EtOH). The yellow solid was Soxhlet extracted in EtOH for 24 h and dried under 100 °C vacuum to afford HIAM-0026 (12.5 mg, yield: 56.6%).

Synthesis of HIAM-0026*v*

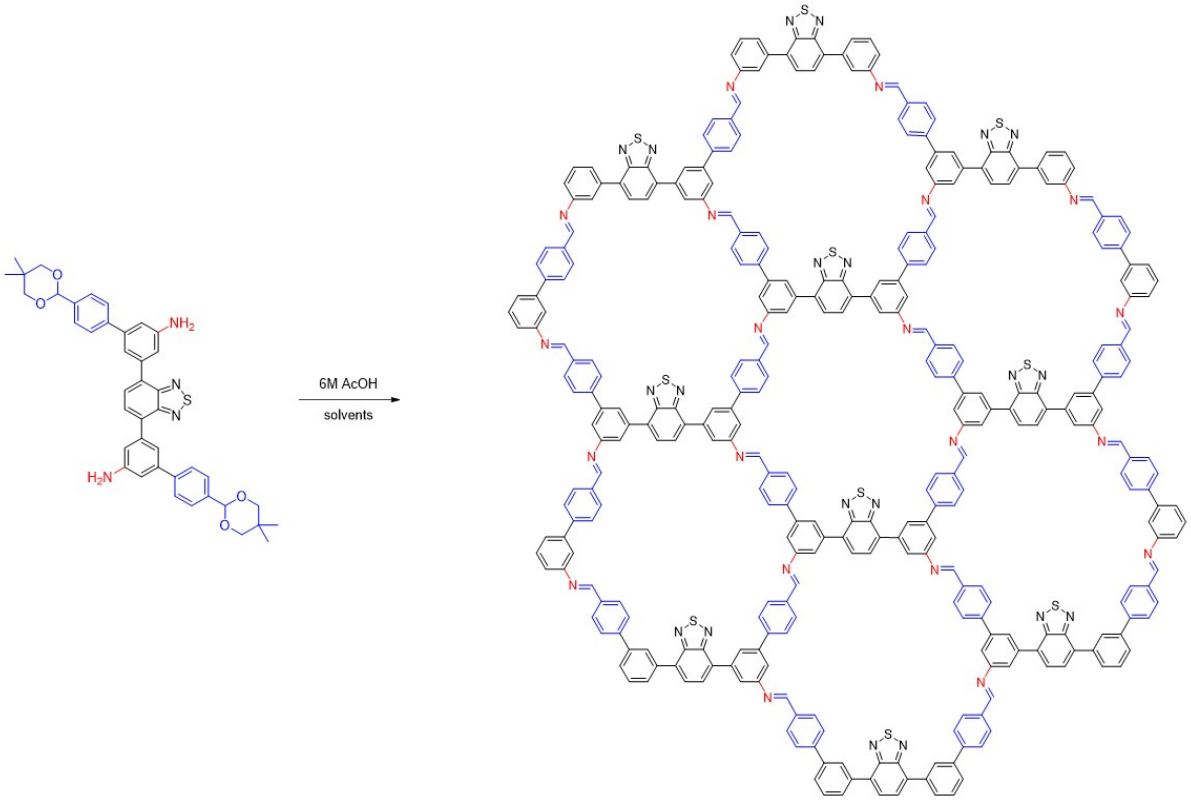

A Pyrex tube (10 mL) containing BTBBA*v* (31.4 mg, 0.045 mmol) and *n*-BuOH (1 mL) was sonicated for 3 min. Subsequently, 0.8 mL of acetic acid (6 M) was added. The tube was degassed through three freeze-pump-thaw cycles and then heated at 120 °C for 72 h. After cooling to room temperature, the precipitate was collected by filtration and washed with DMF and EtOH. The yellow solid was Soxhlet extracted in EtOH for 24 h and dried under 100 °C vacuum to afford HIAM-0026*v* (18.7 mg, yield: 85.0%).

.

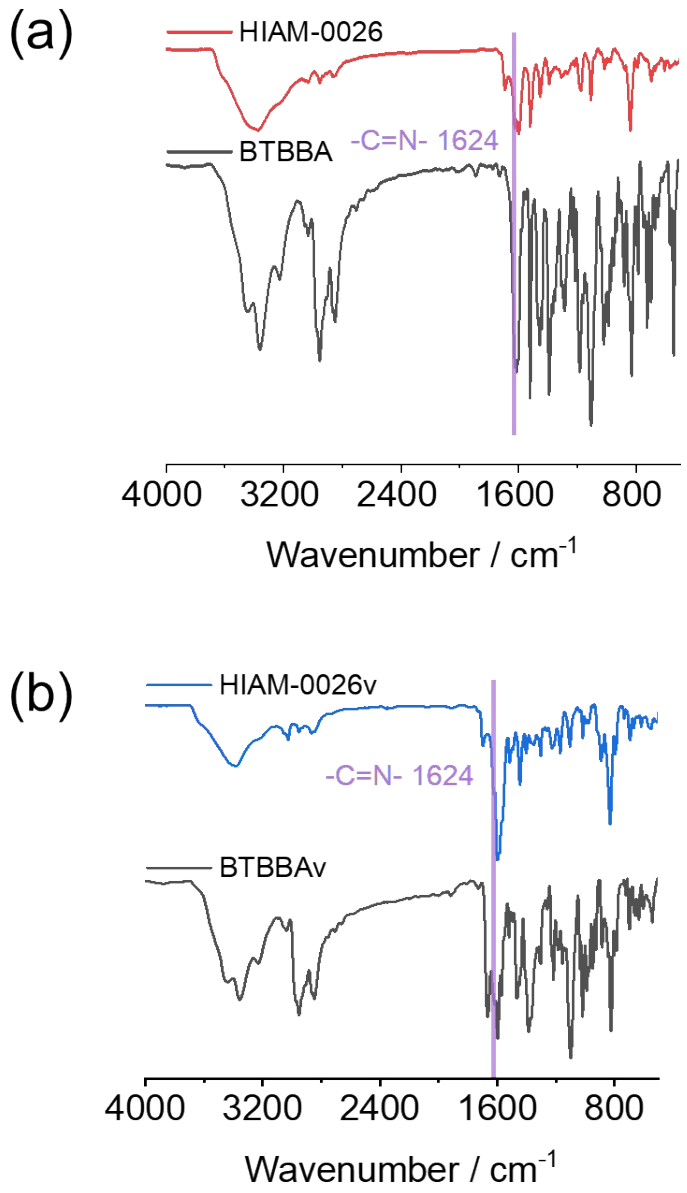

Figure S9. FT-IR spectra of HIAM-0026 (a) and HIAM-0026*v* (b) and the corresponding organic building units.

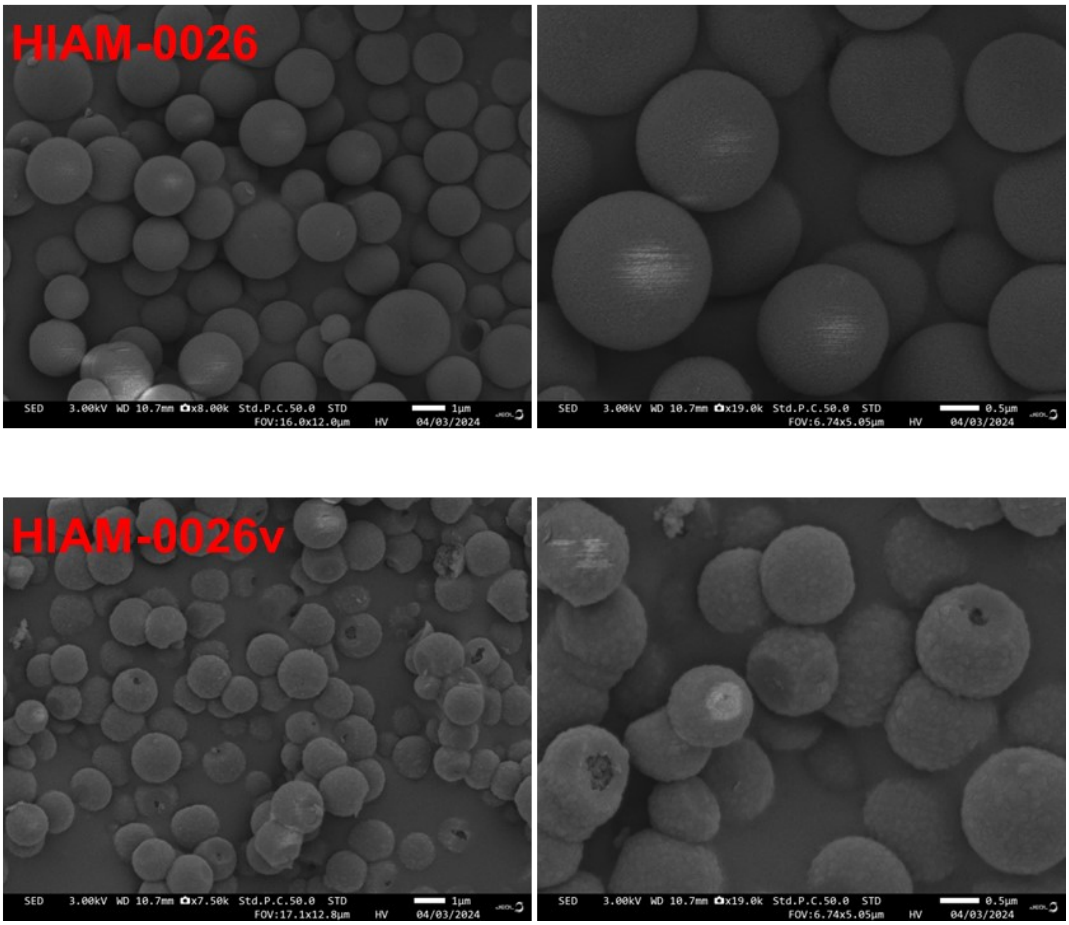

Figure S10. SEM images of HIAM-0026 and HIAM-0026*v*.

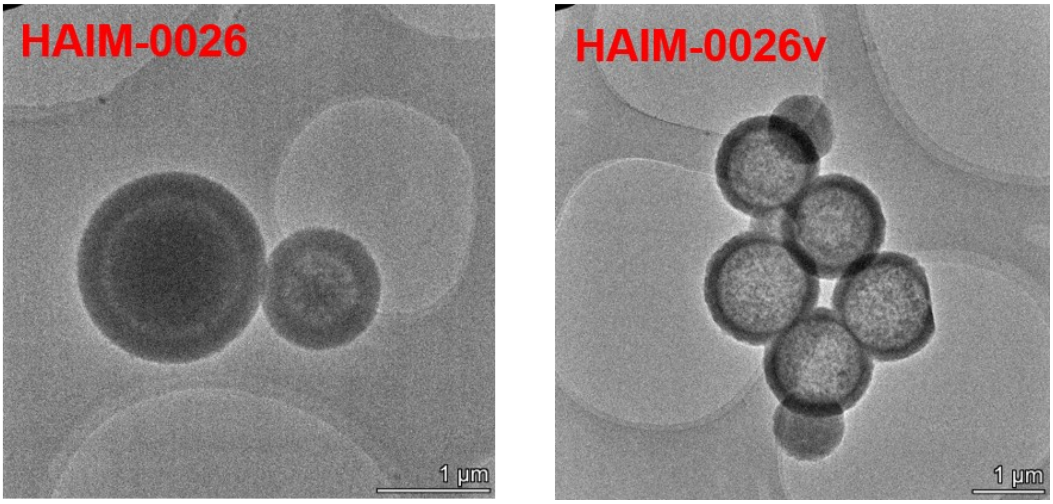

Figure S11. TEM images of HIAM-0026 and HIAM-0026*v*.

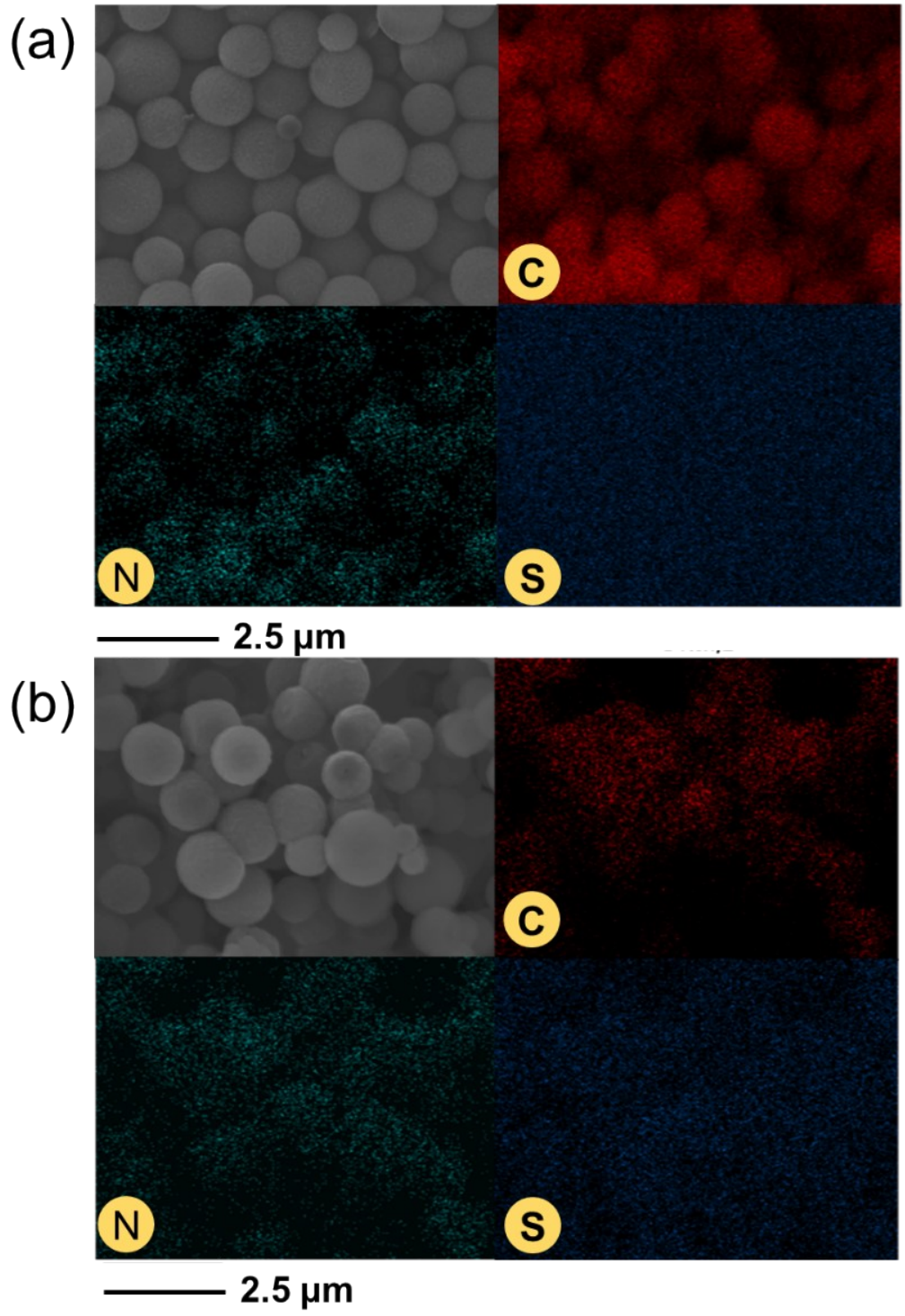

Figure S12. Energy dispersive X-ray analysis of HIAM-0026 (a) and HIAM-0026*v* (b).

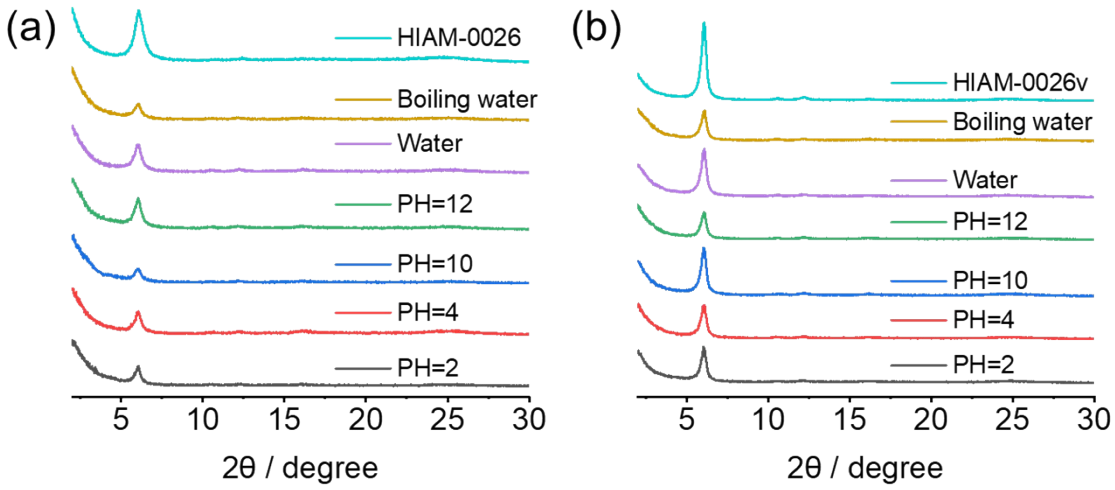

Figure S13. The PXRD patterns of HIAM-0026 (a) and HIAM-0026*v* after treatment under various conditions for 24 hours.

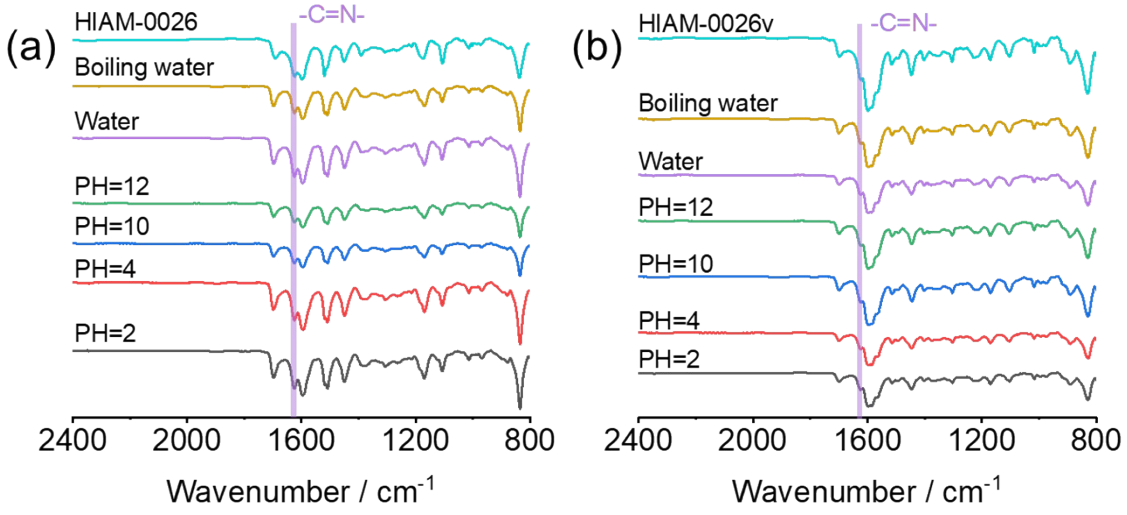

Figure S14. The FT-IR spectra of HIAM-0026 (a) and HIAM-0026*v* after treatment under various conditions for 24 hours.

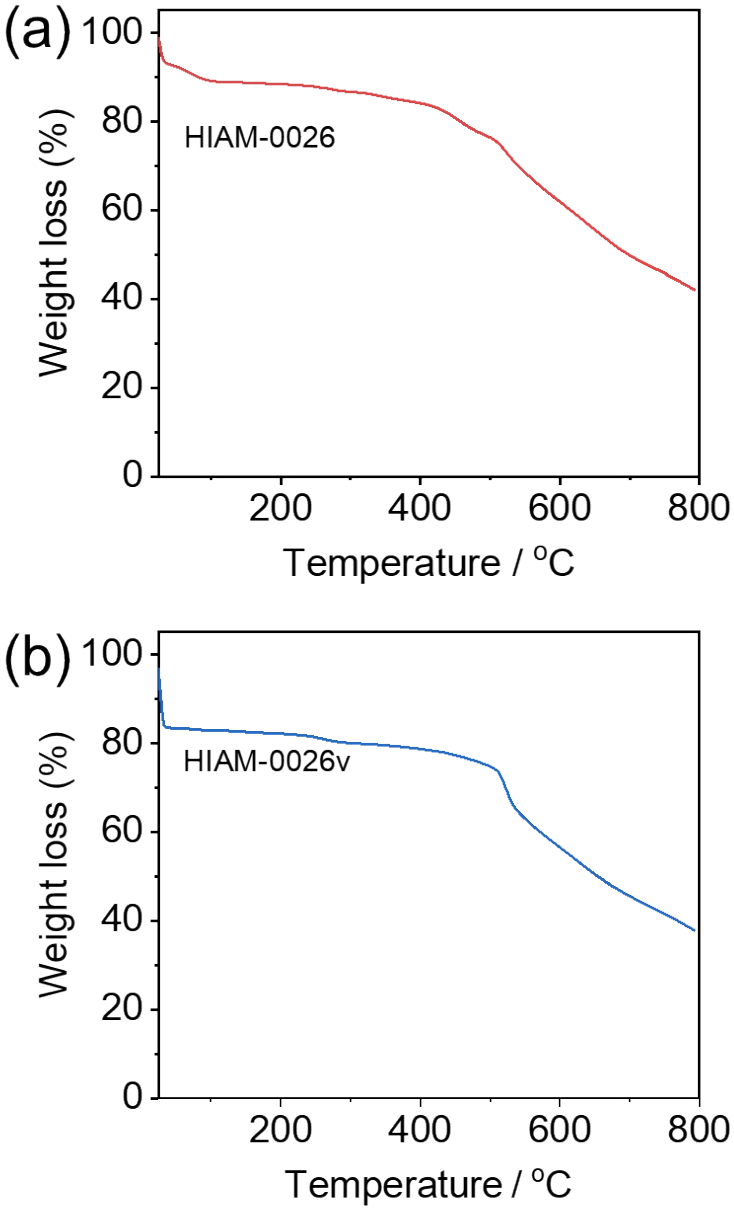

Figure S15. TGA curves of HIAM-0026 (a) and HIAM-0026*v* (b).

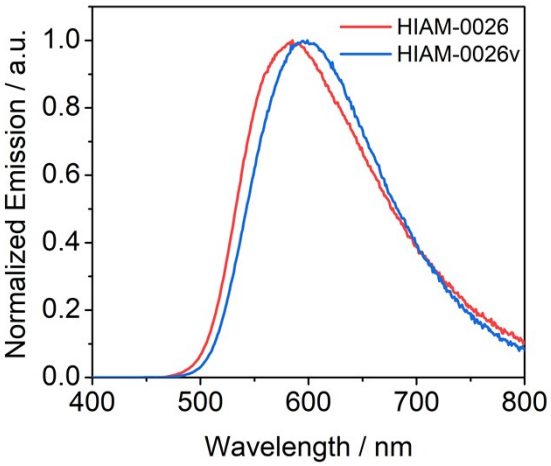

Figure S16. The photoluminescence spectra of HIAM-0026 and HIAM-0026*v*.

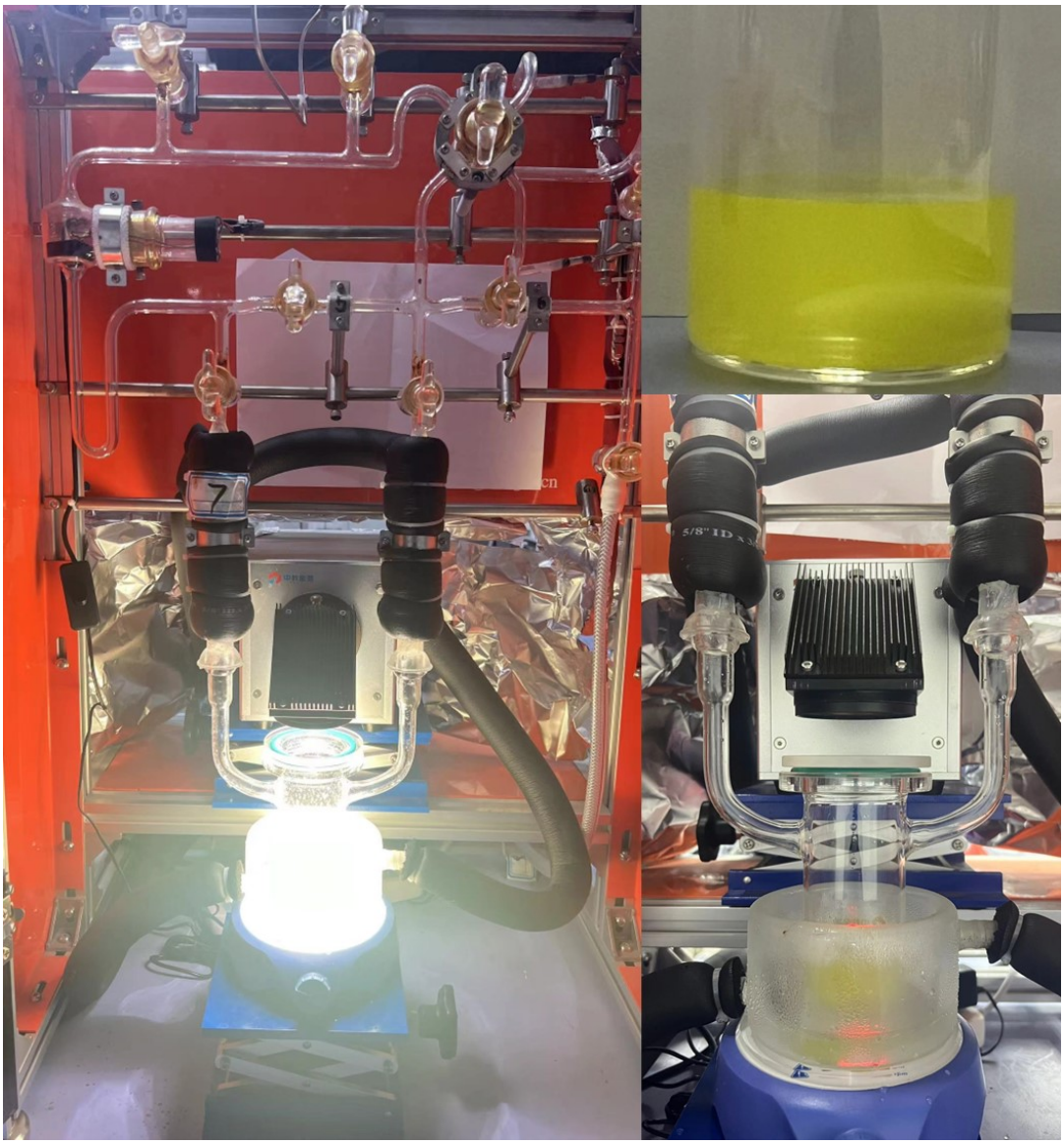

Figure S17. The images of the experimental setup used for the photocatalytic hydrogen generation.

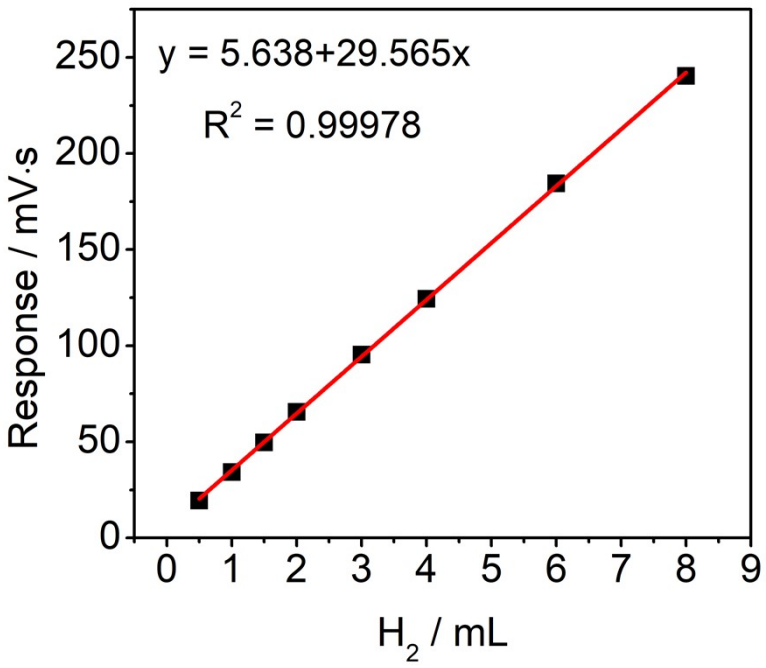

Figure S18. The calibration curve used for the quantification of hydrogen gas.

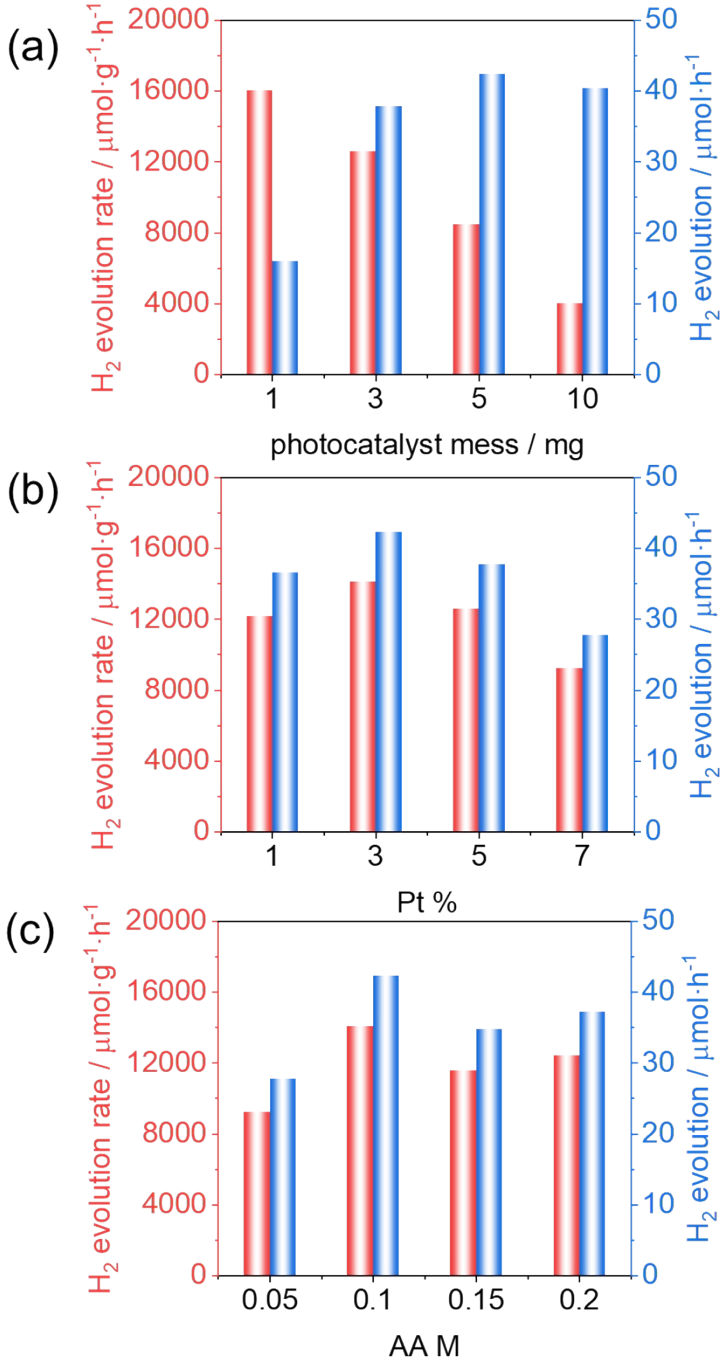

Figure S19. The photocatalyst mass (a), the amount of co-catalyst (b) and concentration of AA (c) effect on the photocatalytic hydrogen performance of HIAM-0026.

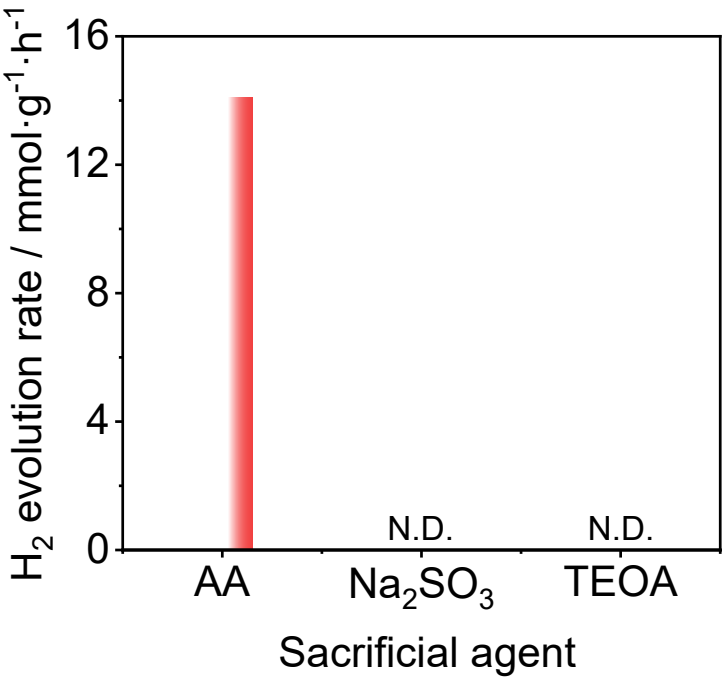

Figure S20. The photocatalytic hydrogen production performance of HIAM-0026 with various sacrificial donors.

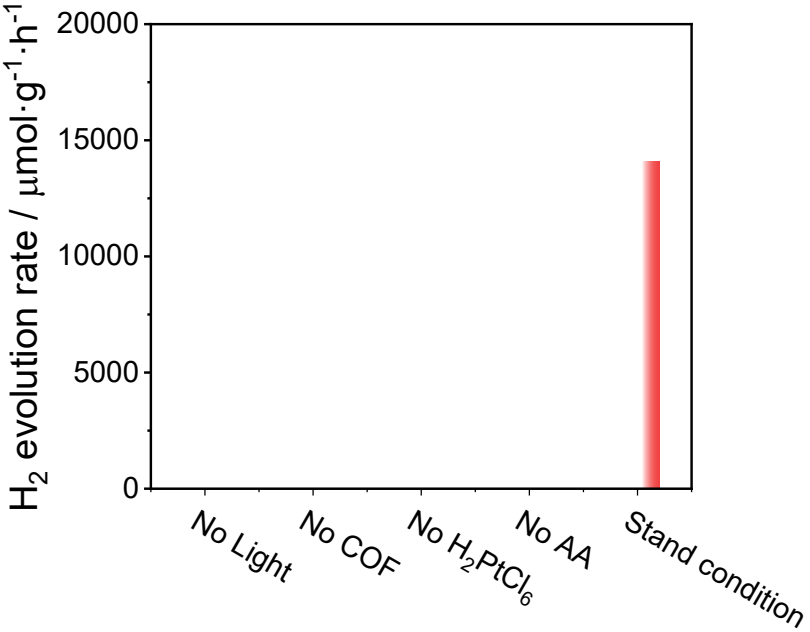

Figure S21. The control experiments of photocatalytic H_2 evolution using HIAM-0026 as the photocatalysts.

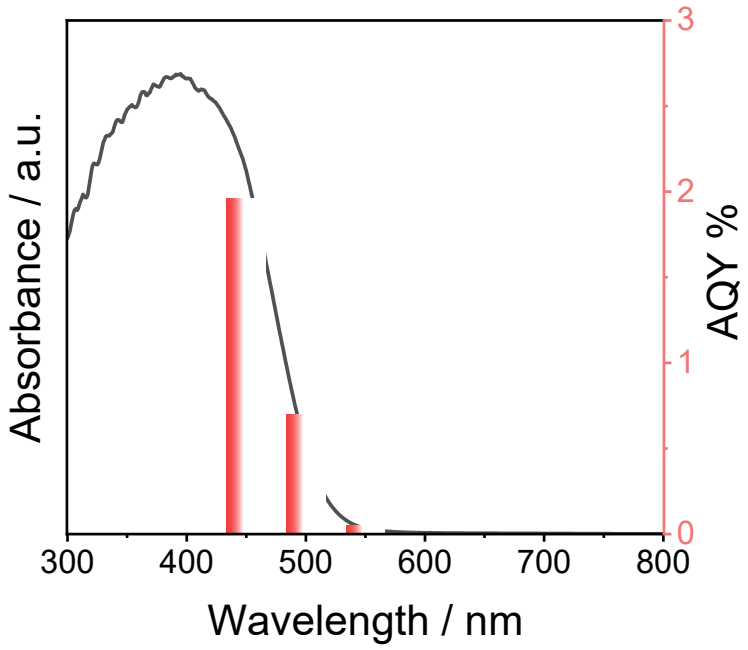

Figure S22. The wavelength-dependent AQY of photocatalytic H_2 evolution for HIAM-0026.

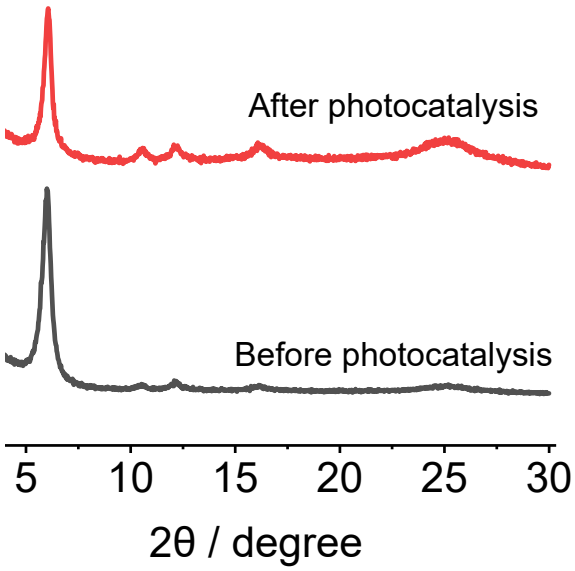

Figure S23. The PXRD patterns of HIAM-0026 before and after photocatalytic measurement.

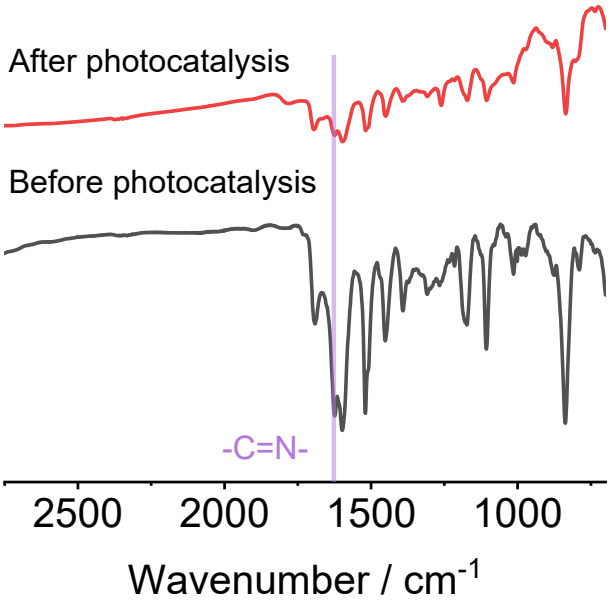

Figure S24. The FT-IR spectra of HIAM-0026 before and after photocatalytic measurement.

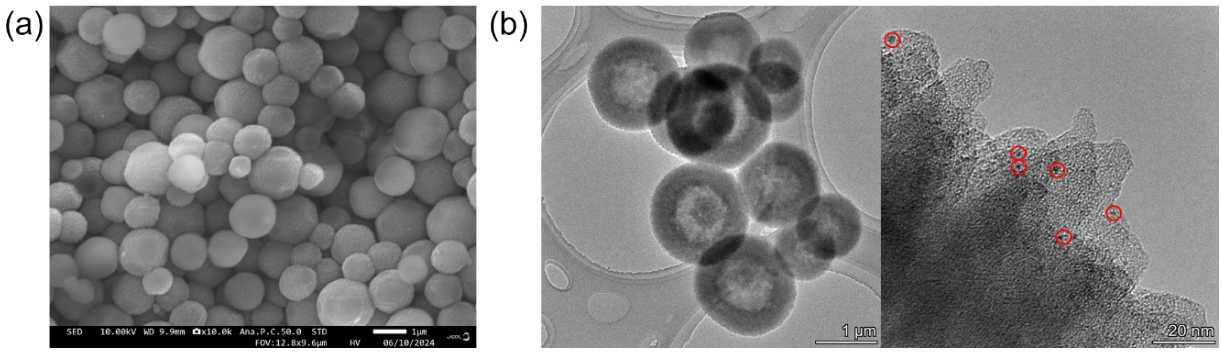

Figure S25. The SEM (a) and TEM (b) images of HIAM-0026 after photocatalytic measurement.

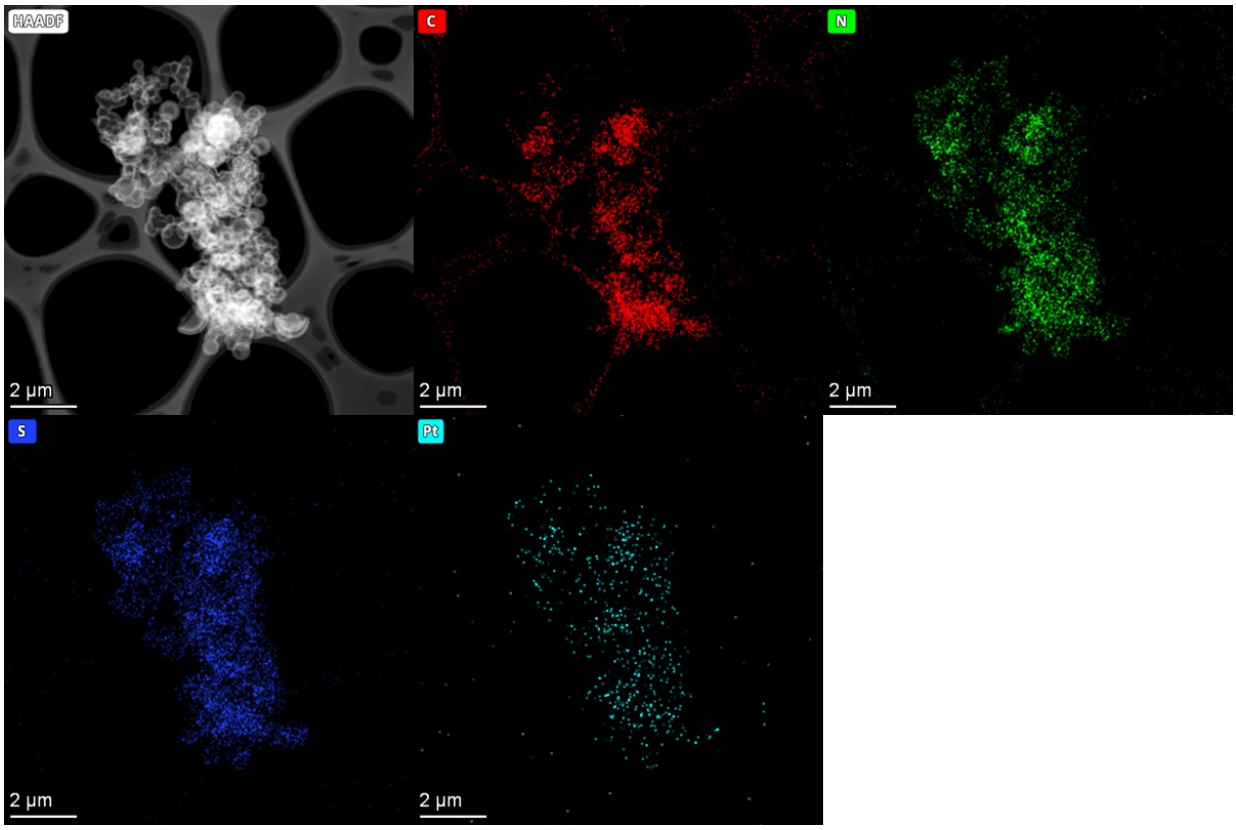

Figure S26. The HAADF-STEM and EDX analysis of HIAM-0026 after photocatalytic measurement.

Table S1. Atomic coordinates of AA-stacking mode of the simulated HIAM-0026.

	Space group: *pm* a = 17.6928 Å, b = 3.3510 Å, and c = 16.6652 Å. α = γ = 90°, and β = 116.7130°		
	Atom	**x**	**y**	**z**
C1	0.47148	-0.00000	0.44363
C2	0.43696	-0.00000	0.34852
C3	0.34776	-0.00000	0.30183
C4	0.29703	-0.00000	0.34556
C5	0.33078	-0.00000	0.43999
C6	0.42082	-0.00000	0.48749
C7	0.48899	-0.00000	0.29655
C8	0.27122	-0.00000	0.48351
C9	0.57903	-0.00000	0.33931
C10	0.62688	-0.00000	0.29105
C11	0.58272	-0.00000	0.19825
C12	0.4958	-0.00000	0.15386
C13	0.4486	-0.00000	0.20134
C14	0.18265	-0.00000	0.43133
C15	0.12868	-0.00000	0.47138
C16	0.16078	-0.00000	0.56427
C17	0.24723	-0.00000	0.6195
C18	0.30074	-0.00000	0.57738
C19	0.72195	-0.00000	0.33505
C20	0.28134	-0.00000	0.72002
C21	0.03771	-0.00000	0.41597
C22	0.45966	-0.00000	0.05665
C23	0.77066	-0.00000	0.42948
C24	0.85858	-0.00000	0.46788
C25	0.8998	-0.00000	0.41373
C26	0.85315	-0.00000	0.32081
C27	0.76642	-0.00000	0.28233
C28	0.22757	-0.00000	0.76298
C29	0.2597	-0.00000	0.85625
C30	0.34629	-0.00000	0.91054
C31	0.40269	-0.00000	0.86625
C32	0.36919	-0.00000	0.77479
N33	0.98935	-0.00000	0.45598
N34	0.37617	-0.00000	1.00099
N35	0.46596	-0.00000	0.57738
S36	0.57662	-0.00000	0.61474

N37	0.55456	-0.00000	0.50026
H38	0.31299	-0.00000	0.23001
H39	0.2305	-0.00000	0.30123
H40	0.61379	-0.00000	0.40945
H41	0.61416	-0.00000	0.15666
H42	0.38134	-0.00000	0.16118
H43	0.15244	-0.00000	0.35928
H44	0.11658	-0.00000	0.59188
H45	0.3653	-0.00000	0.61855
H46	0.01357	-0.00000	0.34393
H47	0.50532	-0.00000	1.03111
H48	0.74353	-0.00000	0.47572
H49	0.89491	-0.00000	0.54031
H50	0.88205	-0.00000	0.27602
H51	0.73828	-0.00000	0.21049
H52	0.15971	-0.00000	0.72703
H53	0.21653	-0.00000	0.88614
H54	0.47068	-0.00000	0.9002
H55	0.4162	-0.00000	0.75087

Table S2. Atomic coordinates of AA-stacking mode of the simulated HIAM-0026*v*.

Space group: *pm* a = 16.7604 Å, b = 3.4336 Å, and c = 17.6106 Å. α = γ = 90°, and β =115.2181°			
Atom	**x**	**y**	**z**
C1	0.46804	-0.00000	0.42068
C2	0.42437	-0.00000	0.33134
C3	0.33152	-0.00000	0.29732
C4	0.28575	-0.00000	0.34732
C5	0.3287	-0.00000	0.43611
C6	0.42237	-0.00000	0.47062
C7	0.47066	-0.00000	0.27299
C8	0.27482	-0.00000	0.48786
C9	0.56377	-0.00000	0.30419
C10	0.60799	-0.00000	0.2523
C11	0.55634	-0.00000	0.16636
C12	0.46434	-0.00000	0.13093
C13	0.42215	-0.00000	0.18417
C14	0.18218	-0.00000	0.44851
C15	0.13164	-0.00000	0.49457
C16	0.17248	-0.00000	0.58135
C17	0.26438	-0.00000	0.62473
C18	0.31341	-0.00000	0.57639
C19	0.70752	-0.00000	0.28649
C20	0.30927	-0.00000	0.71939
N21	0.03758	-0.00000	0.45588
N22	0.41254	-0.00000	0.04103
C23	0.76222	-0.00000	0.37388
C24	0.85354	-0.00000	0.4043
C25	0.89309	-0.00000	0.34867
C26	0.84124	-0.00000	0.2629
C27	0.75044	-0.00000	0.23206
C28	0.26101	-0.00000	0.76905
C29	0.30408	-0.00000	0.85673
C30	0.39596	-0.00000	0.89647
C31	0.44413	-0.00000	0.84871
C32	0.40226	-0.00000	0.76244
C33	0.98822	-0.00000	0.37813
C34	0.44676	-0.00000	0.9871
N35	0.47597	-0.00000	0.55311
S36	0.58926	-0.00000	0.5755

N37	0.55594	-0.00000	0.46584
H38	0.29036	-0.00000	0.23104
H39	0.21548	-0.00000	0.31211
H40	0.60388	-0.00000	0.36855
H41	0.58846	-0.00000	0.12685
H42	0.35139	-0.00000	0.15318
H43	0.14806	-0.00000	0.3822
H44	0.1298	-0.00000	0.61285
H45	0.38168	-0.00000	0.60876
H46	0.73758	-0.00000	0.42111
H47	0.89305	-0.00000	0.47154
H48	0.8711	-0.00000	0.21908
H49	0.71777	-0.00000	0.16482
H50	0.19014	-0.00000	0.74246
H51	0.26576	-0.00000	0.89309
H52	0.51565	-0.00000	0.8783
H53	0.44663	-0.00000	0.73301
H54	0.01284	-0.00000	0.32966
H55	0.51642	-0.00000	1.00573

Table S3. The summary of benzothiadiazole-based COFs for photocatalytic hydrogen generation performance.

COFs	illumination	sacrificial agent	co-catalyst	AQY (%)	H_2 Evolution Rate ($mmol \cdot g^{-1} \cdot h^{-1}$)	Ref
CTF-BT/Th-1	λ≥420 nm	TEOA	3 wt% Pt	7.3 (420 nm)	6.6	1
BT-TAPT-COF	λ≥420 nm	AA	8 wt% Pt	0.19 (410 nm)	0.949	2
Py-ClTP-BT-COF	λ＞420 nm	AA	5 wt% Pt	8.45 (420 nm)	8.875	3
Py-FTP-BT-COF	λ＞420 nm	AA	5 wt% Pt	--	2.875	
Py-HTP-BT-COF	λ＞420 nm	AA	5 wt% Pt	--	1.078	
COF-F	AM 1.5	AA	3 wt% Pt	0.29 (500 nm)	10.581	4
COF-Cl	AM 1.5	AA	3 wt% Pt	--	5.838	
COF-H	AM 1.5	AA	3 wt% Pt	--	5.034	
BTCOF150	λ≥400 nm	TEOA	1 wt% Pt	0.4 (420 nm)	0.75	5
NKCOF-108	λ＞420 nm	AA	5 wt% Pt	5.92 (520 nm)	11.6	6
30%PEG@BT-COF	λ＞420 nm	AA	3.7 wt% Pt	11.2 (520 nm)	11.14	7
USTB-7	λ≥420 nm	AA	3 wt% Pt	--	4.3	8
USTB-8	λ≥420 nm	AA	3 wt% Pt	--	13.7	
TeTz-COF1	λ＞420 nm	AA	4 wt% Pt	3.5 (475 nm)	2.103	9
HPT-COF	λ≥420 nm	AA	3 wt% Pt	--	3.8	10
BT-COF	λ≥420 nm	AA	3 wt% Pt	--	0.68	
HIAM-0001	λ＞420 nm	AA	5 wt% Pt	--	1.41	11
		TEOA	12 wt% Pt	--	1.217	
Py-N-DBT-COF	λ＞420 nm	AA	5 wt% Pt	--	0.82	12
Py-C-DBT-COF	λ＞420 nm	AA	5 wt% Pt	8.65 (450 nm)	21.37	
HIAM-0011	λ＞420 nm	AA	1 wt% Pt	9 (450 nm)	16.98	13
HIAM-0026	λ＞420 nm	AA	3 wt% Pt	1.96 (450 nm)	14.09	This work

References

[1] W. Huang, Q. He, Y. Hu, Y. Li, *Angewandte Chemie International Edition* **2019**, *58*, 8676-8680.

[2] G.-B. Wang, S. Li, C.-X. Yan, Q.-Q. Lin, F.-C. Zhu, Y. Geng, Y.-B. Dong, *Chemical Communications* **2020**, *56*, 12612-12615.

[3] W. Chen, L. Wang, D. Mo, F. He, Z. Wen, X. Wu, H. Xu, L. Chen, *Angewandte Chemie International Edition* **2020**, *59*, 16902-16909.

[4] M. Wang, Z. Wang, M. Shan, J. Wang, Z. Qiu, J. Song, Z. Li, *Chemistry of Materials* **2023**, *35*, 5368-5377.

[5] S. Ghosh, A. Nakada, M. A. Springer, T. Kawaguchi, K. Suzuki, H. Kaji, I. Baburin, A. Kuc, T. Heine, H. Suzuki, R. Abe, S. Seki, *Journal of the American Chemical Society* **2020**, *142*, 9752-9762.

[6] Z. Zhao, Y. Zheng, C. Wang, S. Zhang, J. Song, Y. Li, S. Ma, P. Cheng, Z. Zhang, Y. Chen, *ACS Catalysis* **2021**, *11*, 2098-2107.

[7] T. Zhou, L. Wang, X. Huang, J. Unruangsri, H. Zhang, R. Wang, Q. Song, Q. Yang, W. Li, C. Wang, K. Takahashi, H. Xu, J. Guo, *Nature Communications* **2021**, *12*, 3934.

[8] W. Li, X. Ding, B. Yu, H. Wang, Z. Gao, X. Wang, X. Liu, K. Wang, J. Jiang, *Advanced Functional Materials* **2022**, *32*, 2207394.

[9] L. Hao, K. Huang, N. Wang, R. Shen, S. Chen, W. Bi, N. Li, P. Zhang, Y. Li, X. Li, *Dalton Transactions* **2022**, *51*, 14952-14959.

[10] C. Lin, X. Liu, B. Yu, C. Han, L. Gong, C. Wang, Y. Gao, Y. Bian, J. Jiang, *ACS Applied Materials & Interfaces* **2021**, *13*, 27041-27048.

[11] C.-Q. Han, X. Sun, X. Liang, L. Wang, H. Hu, X.-Y. Liu, *Journal of Materials Chemistry C* **2023**, *11*, 12000-12006.

[12] X. Ren, J. Sun, Y. Li and F. Bai, *Nano Research*, **2024**, *17*, 4994-5001.

[13] J.-X. Guo, Z.-Y. Wang, C.-Q. Han, S. Sun, L. Wang, G. Lu, X.-Y. Liu, *Journal of Materials Chemistry C*, **2024**, *12*, 7741-7747.